Separation Science and Technology
Publication details, including instructions for authors and subscription information:
http://www.informaworld.com/smpp/title~content=t713708471

Operation of an Industrial SMB Unit for *p-xylene* Separation Accounting for Adsorbent Ageing Problems

Pedro Sá Gomes[a]; Mirjana Minceva[a]; Alírio E. Rodrigues[a]
[a] Laboratory of Separation and Reaction Engineering, Associate Laboratory LSRE/LCM Department of Chemical Engineering, Faculty of Engineering, University of Porto, Porto, Portugal

To cite this Article Gomes, Pedro Sá , Minceva, Mirjana and Rodrigues, Alírio E.(2008) 'Operation of an Industrial SMB Unit for *p-xylene* Separation Accounting for Adsorbent Ageing Problems', Separation Science and Technology, 43: 8, 1974 — 2002

To link to this Article: DOI: 10.1080/01496390802064125

URL: http://dx.doi.org/10.1080/01496390802064125

Separation Science and Technology, 43: 1974–2002, 2008

ISSN: 0149-6395 print/1520-5754 online
DOI: 10.1080/01496390802064125

Operation of an Industrial SMB Unit for *p-xylene* Separation Accounting for Adsorbent Ageing Problems

Pedro Sá Gomes, Mirjana Minceva, and Alírio E. Rodrigues
Laboratory of Separation and Reaction Engineering, Associate Laboratory
LSRE/LCM Department of Chemical Engineering, Faculty of Engineering,
University of Porto, Porto, Portugal

Abstract: The industrial separation of p-xylene was considered by means of a standard SMB (Simulated Moving Bed) system as well as the Varicol mode of operation. Both modes of operation were simulated accounting for adsorbent capacity decline using the TMB (True Moving Bed) approach in the case of standard SMB and by a TMB with a non-integer number of columns per section in the Varicol case. Additionally, the TMB model takes into account variable fluid velocity due to the adsorption/desorption rate of p-xylene and its isomers. Dynamic results were used to study the influence of the adsorbent capacity decline on the SMB unit performances and two different compensating measures were tested for a 10 years period: (i) switching time decrease (solid flowrate increase) and (ii) columns redistribution. Both strategies kept the initial purity requirements and reached higher productivity values than the respective unit working without any compensation measure. The switching time compensating strategy proved to be more efficient than the second one, achieving, for the same purity requirements, higher productivity values.

Keywords: Adsorbent; Ageing; Deactivation; Modelling; p-xylene; Separation; Simulated moving bed; Simulation; True moving bed

Received 7 November 2007; accepted 21 January 2008.

Address correspondence to Alirio E. Rodrigues, Laboratory of Separation and Reaction Engineering, Associate Laboratory LSRE/LCM Department of Chemical Engineering, Faculty of Engineering, University of Porto, Rua Dr. Roberto Frias, 4200-465 Porto, Portugal. Tel.: +351 22 5081671; Fax: +351 22 5081674; E-mail: arodrig@fe.up.pt

INTRODUCTION

The Simulated Moving Bed (SMB) technology is an original chromatographic mode of operation that solved several problems usually associated with solid phase motion (particle attrition and wall abrasion, particle size redistribution, increase in pressure drop), present in the continuous counter current adsorptive separation process, the so-called True Moving Bed (TMB). The origins of SMB can be tracked back to early 1960s, and its first relevant industrial implementation to the Sorbex process by Universal Oil Products (1). Since its introduction, the SMB technology has been successfully applied, firstly to various large petrochemical separations, such as the p-xylene separation from its C_8 isomers, n-paraffins from branched and cyclic hydrocarbons, olefins separation from paraffins, the sugar processing industry, and later in the pharmaceutical and fine chemical industries.

As a consequence of this emergent interest, the study and research on this particular topic (mainly in the pharmaceutical and fine chemistry industries), lead to the formulation of quite singular/different operation modes. In particular, the introduction of a nonsynchronous inlet/outlet shift (the Varicol process, (2)), that demonstrated a considerable range of applications extending further the potential of these type of chromatographic techniques (see Appendix for details).

Despite all of the efforts motivated by these applications, the p-xylene separation continues to be the subject of numerous studies and analyses (3–10). This point is understandable given the implementation of new design and process techniques to the so-called "old" SMB applications, which increased raising the performance obtained in these units. Secondly, the actual problematic of oil prices stress and its direct (as a raw material) and indirect influence (energetic source, market dependence...), demanding from the old separation processes more eco-efficient, cleaner, safer, and less energy spending technology. Additionally, there is a growing demand on polymeric materials such as polyester fibers, molded plastics used in films, and blown beverage bottles produced by polyethylene terephthalate (PET), obtained from p-xylene as a raw material. All this interest in the p-xylene production resulted in design and installation of a considerable number of industrial SMB units for p-xylene separation form its C_8 isomers, mainly from UOP (Parex process) and IFP (Eluxyl process).

In the published or patented innovative work related with this fifty years old SMB application to p-xylene separation, just a few references refer to the adsorbent ageing problems (7,11). The information considering this issue remains restricted to the plant operators and technology owners. Generally, the particle size re-distribution and capacity decline as a result of adsorbent ageing are mentioned as possible cause of the SMB performance decline with time.

It is from the common wisdom of the use of guard beds in the gas processing industry in order to prevent the impurities access into the separation process, or more elaborated methods such as online adsorbent removal (12,13) and innovative fluid distribution apparatus (14), to mitigate fine production. Nevertheless, ageing problems such as "parasite" reactions within the solid or liquid phase, and other attrition effects, leading to fine and channelling, occur during the operation of industrial units.

By treating adsorbent ageing as a system disturbance it is possible to compensate it by applying SMB online controllers, as pointed out in recent studies of Morari or Engell research groups (15–17).

However, the implementation of model predictive control methods should also be based on robust ageing models as compensative measures. Additionally, when it comes to design and start-up of a new SMB unit, the analysis of adsorbent ageing factors can have a significant weight on financial and/or management choices involved in these projects. The "time life" of the adsorbent, a predominant economical factor in the SMB units design as adsorbent cost, has considerable influence on the complete unit design, if not in the main project viability.

Therefore, the objective of this work is to present a complete analysis of the adsorbent ageing effect on the performance parameters of an industrial SMB (conventional and Varicol) unit for p-xylene separation, as well as the development of strategies to overcome this problem. This paper is an extension of the general study on SMB adsorbent ageing recently published (11), providing an application to a realistic case which includes a deeper study of the columns rearrangement strategy using dynamic simulations.

MODELLING AND DESIGN STRATEGIES

Case Study: An Industrial Unit for *p-xylene* Separation

The p-xylene system here analysed has been reported by Minceva and Rodrigues in several published works, and represented by the Langmuir Competitive isotherm model:

$$q_{ij}^{*} = \frac{q_{mi} K_i \langle C_{pij} \rangle}{1 + \sum_{l=1}^{Nc} K_l \langle C_{plj} \rangle} \tag{1}$$

where q_{mi} is the adsorbed phase saturation capacity of component *i*, K_i the Langmuir adsorption constant for species *i* and q_{ij}^{*} is the adsorbed phase concentration of component *i* in zone *j* in equilibrium with the

Table 1. Parameters of langmuir adsorption equilibrium isotherms

Component	K_i ($m^3 \cdot kg^{-1}$)	q_{mi} ($kg \cdot kg^{-1}_{adsorbent}$)
(A) p-xylene	1.9409	0.1024
(B) m-xylene	0.8884	0.0917
(C) o-xylene	0.8884	0.0917
(D) ethylbenzene	1.0263	0.0966
(E) p-diethylbenzene	1.2000	0.1010

average pore concentration $\langle C_{pij} \rangle$. The adsorption equilibrium data of the single p-xylene, o-xylene, and ethylbenzene on Ba exchanged faujasite zeolite in liquid phase at 180°C and 9 bar was determined experimentally in a batch mode by Minceva and Rodrigues (9). The adsorption parameters for m-xylene are similar to those for o-xylene in this type of zeolites according to Santacesaria *et al.* (18). The p-DEB isotherm was taken from (19,20). All adsorption equilibrium parameters are presented in Table 1.

The SMB unit geometry design and operating conditions are presented in Table 2, considering constant apparent solid density (ρ_p) and taking into account that the xylenes density (ρ_i) were calculated by means of the commercial flow sheeting package from Aspen (www.aspentech.com) at 180°C and 9 bar.

Mathematical Modelling

As mentioned before, the SMB operating mode appeared as an innovative solution to the majority of the moving bed problems, by simulating

Table 2. Parex unit characteristics and model parameters

Model Parameters	SMB Columns
$Pe_j = 1000$	$N_c = 24$ $n_j = [6\ 9\ 6\ 3]$ *(as reported)*
$\varepsilon_b = 0.387$; $\varepsilon_p = 0.37$	$L_c = 1.135\,m$
$R_p = 0.031\,cm$	$D_c = 4.117\,m$
	SMB Operating Conditions
$\rho_p = 1.480\,g \cdot cm^{-3}$	
$\rho_A = 0.710\,g \cdot cm^{-3}$ $\rho_B = 0.713\,g \cdot cm^{-3}$	$C_A{}^F = 23.6\,wt\%$; $C_B{}^F = 49.7\,wt\%$
$\rho_C = 0.733\,g \cdot cm^{-3}$ $\rho_C = 0.716\,g \cdot cm^{-3}$	$C_C{}^F = 12.7\,wt\%$; $C_D{}^F = 14.0\,wt\%$
$\rho_E = 0.724\,g \cdot cm^{-3}$	$C_E{}^{Desorbent} = 100.0\,wt\%$
$k_{(A,B,C,D)} = 8.1\,min^{-1}$; $k_{(E)} = 6.8\,min^{-1}$	

it with a synchronous shift of the position of all inlet and outlet streams while the solid is kept static. The inlet and outlet streams are the same in both SMB and TMB, establishing four sections, namely: (1) the solid regeneration zone (section 1), placed between the desorbent and extract streams; the separation zones (2) section 2, limited by extract and feed streams; and (3) section 3, limited by feed and raffinate streams; and (4) the eluent regeneration zone (section 4), between the raffinate and eluent streams, Fig. 1.

Given the similarity between the two processes, the SMB and the TMB, it is possible to model an SMB unit based on the TMB *modus operandi*. In fact this kind of approach provides acceptable results when a large number of columns per section is considered (7), saving a considerable computation time, and providing the steady state solutions instead of the cyclic steady sate (CSS) obtained with the SMB models.

Therefore, the TMB modelling approach was used, avoiding a significant computation effort and calculation time. The equivalence between the SMB and the TMB model is established by means of the relation between the SMB average liquid phase interstitial velocity

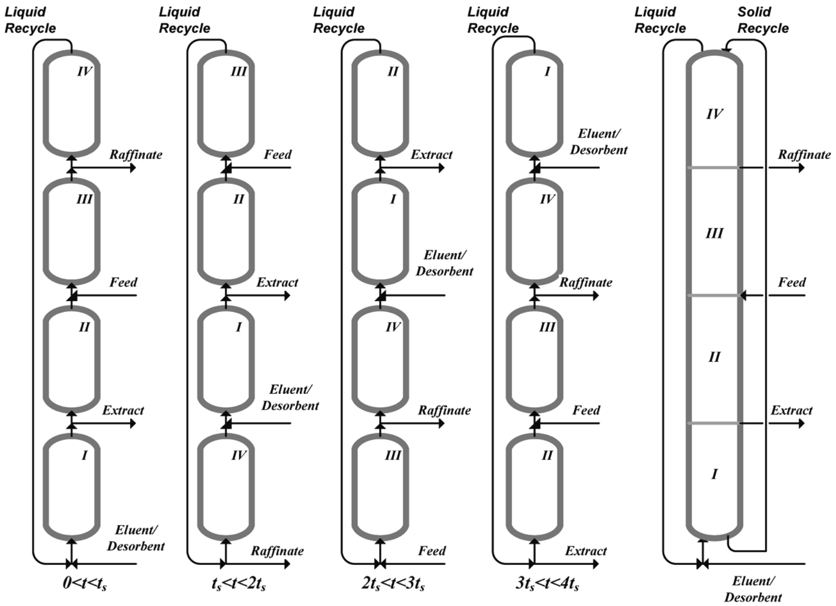

(a) (b)

Figure 1. Scheme of a 4 columns SMB unit operating over a complete cycle from 0 to $4t_s$ (where t_s is the ports switching time) (a), and the equivalent "4 columns length" TMB unit (b).

($\langle u_j^* \rangle$) with the TMB average liquid interstitial velocity ($\langle u_j \rangle$) and the solid interstitial velocity (u_s) in each section j: $\langle u_j^* \rangle = \langle u_j \rangle + u_s$. The model accounts for velocity variations due to adsorption/desorption rates leading to more accurate results (the *p-xylene* and its isomers system should be considered as an high concentration system). The solid velocity in the TMB is calculated as a ratio between the column length (L_c) and the switching time interval (t_s) in the SMB unit: $u_s = L_c/t_s$. Again, the average internal flow-rates in both models are not the same, but related by $\langle Q_j^* \rangle = \langle Q_j \rangle + \varepsilon_b V_c/t_s$, where $\langle Q_j^* \rangle$ and $\langle Q_j \rangle$ are the average internal liquid flow-rates in the SMB and TMB, respectively, V_c is the column volume and ε_b is the bed porosity. Respecting the section nodes balances:

$$\textit{Desorbent node}: C_{bi(4,z=L_4)} = \frac{u_{(1,z=0)}}{u_{(4,z=L_4)}} C_{bi(1,z=0)} - \frac{u_{De}}{u_{(4,z=L_4)}} C_i^{De} \tag{2a1}$$

$$\textit{Extract } (j=2) \textit{ and Raffinate } (j=4) \textit{ nodes}: C_{bi(j-1,z=L_{j-1})} = C_{bi(j,z=0)} \tag{2a2, 3}$$

$$\textit{Feed node}: C_{bi(2,z=L_2)} = \frac{u_{(3,z=0)}}{u_{(2,z=L_2)}} C_{bi(3,z=0)} - \frac{u_F}{u_{(2,z=L_2)}} C_i^{F} \tag{2a4}$$

and,

$$u_{(1,z=0)} = u_{(4,z=L_4)} + u_{De} \quad \textit{Desorbent (De) node}; \tag{2b1}$$

$$u_{(2,z=0)} = u_{(1,z=L_1)} - u_X \quad \textit{Extract (X) node}; \tag{2b2}$$

$$u_{(3,z=0)} = u_{(2,z=L_2)} + u_F \quad \textit{Feed (F) node}; \tag{2b3}$$

$$u_{(4,z=0)} = u_{(3,z=L_3)} - u_R \quad \textit{Raffinate (R) node}. \tag{2b4}$$

The TMB model assumes: convective axial dispersed liquid flow, with variable velocity, flowing counter currently to the solid plug flow; homogeneous particles with constant radius R_P; constant axial dispersion and intraparticle mass transfer resistances; and negligible pressure drops and thermal effects.

The mass balance for the component i in the bulk fluid phase:

$$\frac{\partial C_{bij}}{\partial t} = D_{ax}\frac{\partial^2 C_{bij}}{\partial z^2} - \frac{\partial (C_{bij}u_j)}{\partial z} - \frac{(1-\varepsilon_b)}{\varepsilon_b} k_{ij}(C_{bij} - \langle C_{pij} \rangle) \tag{3}$$

The particle mass balance for component i:

$$\rho_p \frac{\partial q_{ij}}{\partial t} + \varepsilon_p \frac{\partial \langle C_{pij} \rangle}{\partial t} = u_s \left\{ \rho_p \frac{\partial q_{ij}}{\partial z} + \varepsilon_p \frac{\partial \langle C_{pij} \rangle}{\partial z} \right\} + k_{ij}(C_{bij} - \langle C_{pij} \rangle) \tag{4}$$

With the initial and boundary conditions:

$$\begin{cases} C_{bij}(z,0)=0; \\ \langle C_{pij}(z,0)\rangle = 0; \quad i=(A,B,C,D) \\ \langle q_{ij}(z,0)\rangle = 0; \end{cases} \quad \text{and} \quad \begin{cases} C_{bEj}(z,0)=\rho_E; \\ \langle C_{pEj}(z,0)\rangle = \rho_E; \\ \langle q_{Ej}(z,0)\rangle \cong q_{m_E}; \end{cases} \tag{5}$$

$$z=0: C_{bi(j,z=0)} = C_{bij}(0,t) - \frac{D_{ax}}{u_j}\frac{\partial C_{bij}}{\partial z}\bigg|_{z=0} \tag{6}$$

$$z=L_j: \frac{\partial C_{bij}}{\partial z}\bigg|_{z=L_j} = 0 \tag{7}$$

and

$$z=L_j: \begin{cases} \langle C_{pij}\rangle = \langle C_{pi(j+1,z=0)}\rangle, \quad \text{for } j=1,2,3; \\ \langle C_{pi4}\rangle = \langle C_{pi(1,z=0)}\rangle \end{cases} \tag{8}$$

$$z=L_j: \begin{cases} q_{ij} = q_{i(j+1,z=0)}, \quad \text{for } j=1,2,3; \\ q_{i4} = q_{i(1,z=0)} \end{cases} \tag{9}$$

The adsorption equilibrium isotherm defined as:

$$q^*_{ij} = f_i(C_{pij}, C_{plj}) \text{ with } l \neq i \text{ and for all species } i \text{ and in section } j \tag{10}$$

Since the pressure drops were assumed to be negligible, it is considered that:

$$\sum_{i=1}^{NC} \frac{C_{bij}}{\rho_i} = 1$$

It is possible to calculate the interstitial fluid velocity by means of the total mass balance:

$$\frac{du_j}{dz} = -\frac{(1-\varepsilon_b)}{\varepsilon_b}\sum_{i=1}^{NC}\frac{k_{ij}}{\rho_i}(C_{bij} - \langle C_{pij}\rangle)$$

where C_i^F the species i concentration in the feed, $C_{bij}, \langle C_{pij}\rangle$, q_{ij} the bulk, the average pore and the adsorbed concentration, respectively, t is the temporal coordinate, z is the axial coordinate, L_j is the section length and k_{ij} is the particle mass transfer coefficient.

The Varicol mode of operation, characterized by an asynchronous ports shift, was also studied on this work and for the sake of simplicity, modelled by means of an equivalent TMB unit working with a non integer number of columns per section. In the limit we consider that a Varicol unit with infinite number of columns and infinite number of sub-switching-intervals within the principal switching time interval, is equivalent to the mentioned TMB unit (with non integer number of columns per section, or different columns length), see Appendix.

Performance Parameters

The commonly used SMB unit performance parameters are: purity, recovery, desorbent consumption and productivity. The SMB outlet streams must satisfy purity and recovery specifications. The definitions of extract purity (PUX, %), raffinate purity (PUR, %), recovery of p-xylene in the extract (REX^A, %) and the unit productivity in terms of p-xylene in the extract (PR_X^A), obtained by the TMB model approach at steady-state are:

$$PUX^A(\%) = \frac{C_{b_A}^X}{C_{b_A}^X + C_{b_B}^X + C_{b_C}^X + C_{b_D}^X} \times 100 \tag{11a}$$

$$REX^A(\%) = \frac{Q_X C_{b_A}^X}{Q_F C_A^F} \times 100 \tag{11b}$$

$$PR_X^A = \frac{Q_X C_{b_A}^X}{V_{realsolid}} = \frac{REX^A \cdot Q_F C_A^F}{V_{realsolid}} \tag{11c}$$

where Q_X and Q_F are the extract and feed flow rates, respectively and V_{ads} is the adsorbent volume.

Numerical Solution

The TMB model, constituted by systems of PDE (Partial Differential Equations), ODE (Ordinary Differential Equations) and AE (Algebraic Equations), was numerically solved using the commercial package gPROMS v.3.0.3 (www.psenterprise.com), using the Orthogonal Collocation on Finite Elements (OCFEM) discretization methods for the axial domain (with 2 collocation points per element, 50 elements in each section). After the axial discretization step, the time integration is performed by the ordinary differential equation solver SRADAU, a fully-implicit Runge-Kutta method that implements a variable time step, the resulting system is then solved by the gPROMS BDNSOL (Block decomposition NonLinear SOLver). For all simulations was set a tolerance value equal to 10^{-5}.

For the optimization procedure it was used one of the optimization algorithms within the gPROMS (gOPT) package, namely: the CVP_SS, a control vector parameterization (CVP) approach which assumes that the time-varying control variables are piecewise-constant (for the Varicol studies) functions of time over a specified number of control intervals, with a "single-shooting" dynamic optimization algorithm (SS).

Optimization of a Conventional SMB unit for *p-xylene* Separation

The optimization problems are usually classified considering the number of objective functions: single or multiple-objective. The objective function could be based on different unit performance parameters (as for example, the productivity, the desorbent consumption (where is implicit the dilution factor, energetic duty for distillation or other process for desorbent recovery, etc.) or the adsorbent requirements) or could be homogenized/normalized into the total separation cost (in this case the function of relative weights given to the different cost factor inherent to the separation cost).

Several optimization studies have been performed considering the p-xylene separation, principally multi-objective ones, accounting for the maximization of SMB unit productivity and minimization of desorbent consumption (6, 21, 22).

Taking into account that the main objective of this study is related to the adsorbent ageing analysis, the optimization procedures were reduced to a single objective function problem: the maximization of unit productivity under a constant desorbent flow rate ($Q_{D_e} = 129.00\,\mathrm{m}^3 \cdot \mathrm{h}^{-1}$), constant adsorbent amount (= 24 columns, column length and diameter given in Table 2) and constrained by the p-xylene purity ($\geq$99.5%) and recovery ($\geq$97.5%) in the extract stream.

Following this procedure the industrial SMB unit for the p-xylene separation with a fresh adsorbent was optimized. The maximum productivity of: $PR_X^A = 120.85 \frac{kg_{p\text{-}xylene}}{hm^3_{realsolid}}\Big|_{TMB}$, with $REX^A = 97.5\%\big|_{TMB}$ and $PUX^A = 99.5\%\big|_{TMB}$ was obtained by optimization of the control variables: the internal (recycle) flow rate, that leaves section 4 to section 1 ($Q_{Rec} = 248.80\,\mathrm{m}^3.\mathrm{h}^{-1}$); the extract flow rate ($Q_{Ext} = 94.39\,\mathrm{m}^3.\mathrm{h}^{-1}$); the feed flow rate ($Q_{Feed} = 103.57\,\mathrm{m}^3.\mathrm{h}^{-1}$) and the switching time ($t_s = 1.04\,\mathrm{min}$), the remaining parameters were calculated from the mass balance taking into account the constant desorbent flow rate as mentioned before. By simulating this solution with the TMB model it was possible to obtain the unit bulk internal concentration profiles presented in Fig. 2.

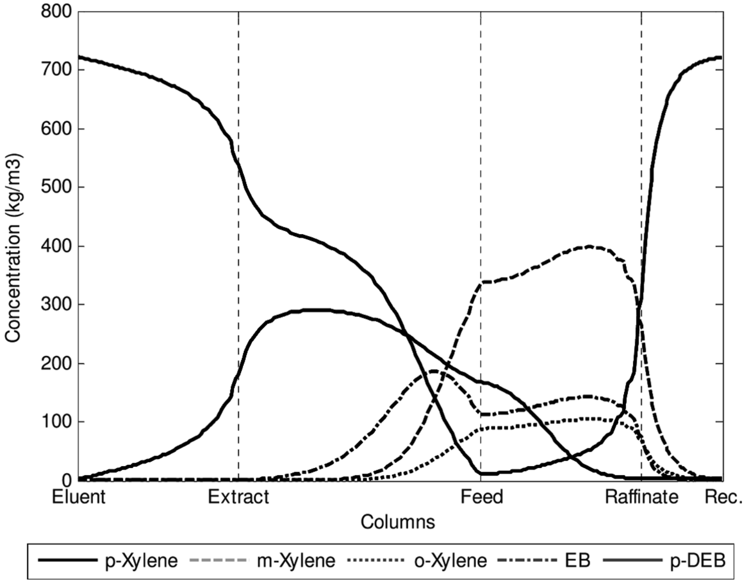

Figure 2. Steady state concentration profiles for a [6 9 6 3] SMB unit simulated by the TMB model approach.

Optimization of Varicol SMB Unit for *p-xylene* Separation

The operation of a p-xylene separation unit by means of a Varicol modus operandi has been studied previously (22). The single objective function problem was considered again, assuming a unit with fresh adsorbent. Namely, maximization of unit productivity under a constant desorbent flow rate ($Q_{De} = 129.00\,\mathrm{m}^3.\mathrm{h}^{-1}$), adsorbent amount (=24 columns, column length, and diameter as in Table 2) and constrained by the p-xylene recovery ($\geq$97.5%) and purity ($\geq$99.5%), but now taking also into account the control variables n_j (number of columns per sections) where $\sum_{j=1}^{NC} n_j = 24$. It was possible to extend the maximum productivity value to: $PR_X^A = 123.89 \frac{kg_{p-xylene}}{hm^3_{realsolid}}\Big|_{TMB}$ (more 2.52 % than the classic unit, an expected result since the classic unit with 24 columns has optimal section lengths, and therefore, there are no considerable improvements with the use of Varicol mode of operation), with $REX^A = 97.6\%|_{TMB}$ and $PUX^A = 99.5\%|_{TMB}$. The following optimal values of the control variables were obtained: the internal recycle flow rate, that leaves section 4 to section 1 ($Q_{Rec} = 267.89\,\mathrm{m}^3.\mathrm{h}^{-1}$); extract flow rate ($Q_{Ext} = 99.96\,\mathrm{m}^3.\mathrm{h}^{-1}$); feed flow rate ($Q_{Feed} = 106.10\,\mathrm{m}^3.\mathrm{h}^{-1}$), and switching time

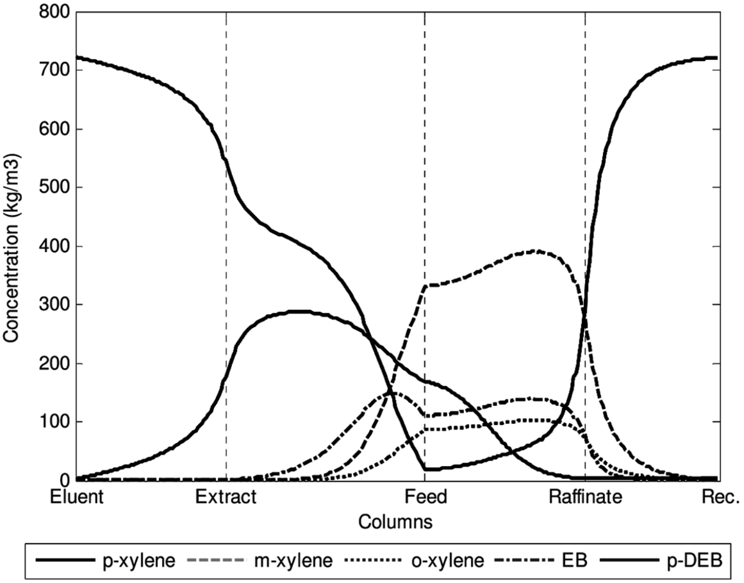

Figure 3. Steady state concentration profiles for Varicol unit simulated by a TMB model approach with configuration of [5.6 7.4 6 5]*.

($t_s = 1.00\,\text{min}$), and column configuration [5.6 7.4 6 5]*, providing the following steady state bulk concentration profiles presented in Fig. 3.

EFFECT OF THE ADSORBENT AGEING ON SMB UNIT PERFORMANCES AND COMPENSATING MEASURES

The operation of SMB units for the separation of p-xylene accounting for ageing effects, adsorbent deactivation or increase of mass transfer resistances, is not a usual issue on the scientific publications, nor mentioned in industrial brochures. Nevertheless, adsorbent deactivation, poisoning, particles crush, particle size redistribution etc are indeed a present problem (23, 24). The use of guard beds, avoiding impurities to enter in the separation process, is one of the more successful as common countermeasures applied. However, some impurities appear/are formed just inside the separation columns in presence of the adsorbent (the presence of oxygenated contaminates in presence of Faujasite zeolites for instance, (25)). One can deal with these aspects by means of online control.

---

*Columns configuration representing a Varicol system as non integer number of columns in an "equivalent" TMB approach.

However, the efficiency of these control routines would be considerably improved by means of short cut routines to these specific problems. Additionally, the initial project of these units should also take into account this "natural" deactivation process inside the columns happening during the unit operation. A previous study on the operation of SMB units in presence adsorbent ageing was recently published (Sá Gomes et al., (11)). A generic study that classifies the adsorbent ageing phenomena into two major classes, according to the consequences observed during unit operation: adsorbent capacity decline and mass transfer resistances increase.

One may argue that in the case of p-xylene separation units the dominant cause for SMB performances decline is due to the adsorbent capacity decline, as pointed out by Minceva and Rodrigues (7) and Yu (23). In particular Yu pointed out two types of adsorbent capacity decline: due to temporary poisoning and permanent one. Additionally, and as pointed out in the introduction, also particle size re-distribution (associated with the pressures variation within the columns during long periods operation), is one of the major concerns in the operation of these type of units. But one can also include its major consequences in a sort of "global adsorbent capacity decline", i.e., the particle crush (as result of pressure variation etc) will manly reduce particles size (the formation of fines), as consequence, one should expect that some parts of the packed column will experience channelling/dead volumes, which we considered as an adsorbent capacity decline (overall is like loosing a part of the available adsorbent).

Minceva and Rodrigues mentioned that usually an industrial p-xylene unit will suffer an adsorbent capacity decline around 20% in 20 years, a permanent capacity decline. The major objective of this work is therefore the study of this permanent capacity decline.

Adsorbent Ageing in a *p-xylene* Separation Unit

Let us consider that an SMB unit for the *p-xylene* separation will lose 20% of its adsorbent capacity during a period of 20 years ($1\% \cdot \text{year}^{-1}$). The unit design should account for it and study what measures could be implemented to maintain the unit operating at acceptable performance parameters (purity, recovery), before complete adsorbent substitution.

In this study the adsorbent capacity decline rate (ξ) is also assumed to be constant at value of $1\% \cdot \text{year}^{-1}$, similar to all species,

$$Q_{mi} = Q_{mi}^{0} \cdot (1 - \xi t) \tag{12}$$

where Q_{mi}^{0} represents the initial adsorption isotherm constant (q_{mi} in Eq. (1)) and t the time variable here in years.

A conventional unit operating with fresh adsorbent for 10 years, as the one set in section on the optimization of the conventional SMB unit, will recover 1.4825 Mton of p-xylene (over a 10 years period), at a purity rate of 99.5% and recovery of 97.5%. If one consider the absorbent capacity decline mentioned above, at the end of the 10th year the unit would recovered just 1.3264 Mton (for a 10 years period) of p-xylene in the extract stream (i.e. less 10.39%) with *p-xylene* purity of 99.0% and recovery of 75.9%. The evolution of the internal bulk concentration profiles after 10 days, after 5 years and after 10 years, without any absorbent capacity decline compensating measure are presented in Fig. 4.

In Fig. 4, one can observe that p-xylene is being driven to the raffinate port over the time of adsorbent ageing, affecting the p-xylene recovery. Therefore, it should be studied how much this separation performances could be improved and which is the countermeasure that should be applied to minimise the adsorbent capacity decline effect.

Similar bulk concentration profiles where obtained for the Varicol operation mode.

A Varicol unit operating with fresh adsorbent for 10 years, as the one set in section on optimization of varicol SMB unit, will recover 1.5198 Mton of *p-xylene* (over a 10 years period), with purity of 99.5% and recovery of 97.6%. If one considers the absorbent capacity decline mentioned above, at the end of the 10th year the unit would recovered just 1.3630 Mton of *p-xylene* (over 10 years) in the extract stream (i.e., less 10.53%) with 99.0% p-xylene purity and 76.0% p-xylene recovery.

Compensating Measures

This study considers the use of compensating measures by which all inlet and outlet SMB streams flow rates are kept unchanged, keeping the auxiliary units (distillation columns, etc) dimensioned as for the initial state. Therefore, three operating parameters can be manipulated as compensating measures:

1. the solid flowrate (switching time);
2. the section length (by means of columns redistribution) and
3. the fluid recycle flowrate.

Sá Gomes et al. (11) stated that both the decrease of recycle flowrate and increase of solid flowrate (decrease of switching time) have similar effect on the operating conditions.

However, the solid flowrate compensation follows the adsorbent decline tendency and the recycle flowrate correction measure will only give results

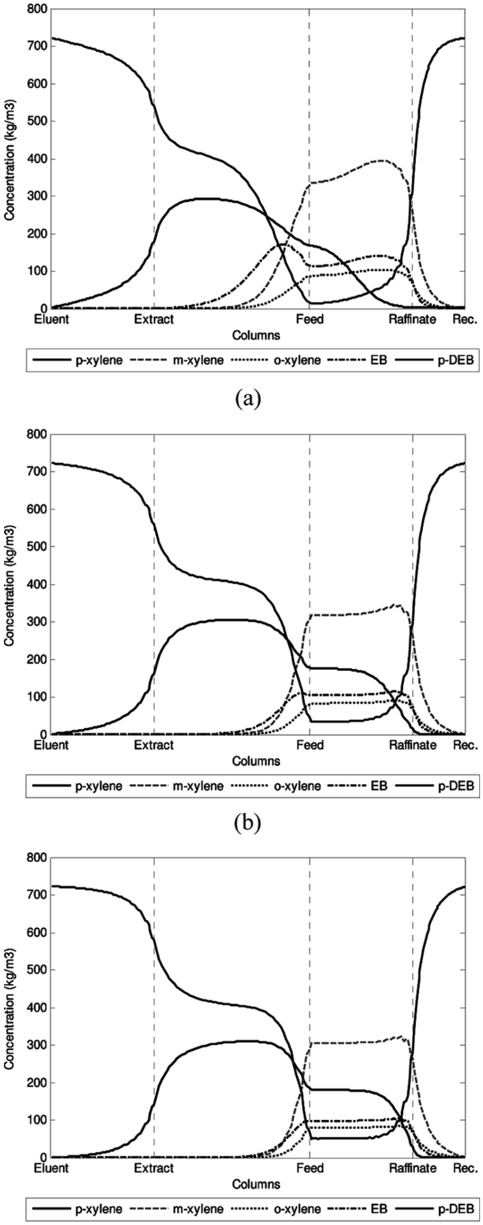

(a)

(b)

(c)

Figure 4. Bulk concentration profiles evolution over a 10 years period without any compensating measure, (a) after 10 days, (b) after 5 years and (c) after 10 years.

in the initial ageing stage. Consequently, just the first two measures are considered in this study (i) and (ii). Additionally both strategies were applied together in a Varicol modus operandi, i.e., a simple extension of strategy (i) to the non-conventional operating mode (Varicol).

Switching Time (Solid Flowrate) Compensation

In Sá Gomes et al. (11) is proposed that if the adsorbent capacity decline rate is similar for all species (linear or non linear isotherms case) then, one simple and straightforward countermeasure is the solid flow rate increase (switching time decrease). The same analysis can be applied to this particular case. In Fig. 5, the influence of the adsorbent capacity decline on the separation region (here defined in terms of $(Q_2 \times Q_3)$ for better understanding and following the nomenclature on the cited paper), shows the same tendency as the ones studied in our previous work (11).

Therefore, for a 10% adsorbent capacity decline one should decrease the switching time by 10%. With a better look on equation (4), and if one considers that the particle porosity is kept constant during the unit operation, it is simple to understand that this countermeasure should be weighted with the porosity information, thus, porosity weight factor α was introduced. Let us assume that the switching time compensation measure for this system is:

$$t_s = t_s^0\left(1 - \frac{1}{\alpha}\xi t\right) \tag{13}$$

where t_s^0 represents the initial time switch value, t the time variable again in years.

A first estimative to the α value can be obtained from a closer look on Eq. (4) and substituting the isotherm information on q_{ij}.

Since the adsorption equilibrium term of species $i\left[\frac{q_{mi}K_i\langle C_{pij}\rangle}{1+\sum_{l=1}^{Nc}K_l\langle C_{plj}\rangle}\right]$ is dependent on average pore concentration, not equal along the SMB unit, let us simplify and assume that:

$$\sum_{l=1}^{Nc} K_l\langle C_{plj}\rangle \approx \overline{K}_i\overline{\langle C_p\rangle}$$

and

$$\begin{cases} \overline{K}_i = K_i\overline{\langle x_{pi}\rangle} \\ \overline{q}_{mi} = q_{mi}\overline{\langle x_{pi}\rangle} \end{cases}$$

where $\overline{K}_i$ and $\overline{q}_{mi}$ represents a weighted average values for the adsorption constant and the adsorbed phase saturation concentration of component

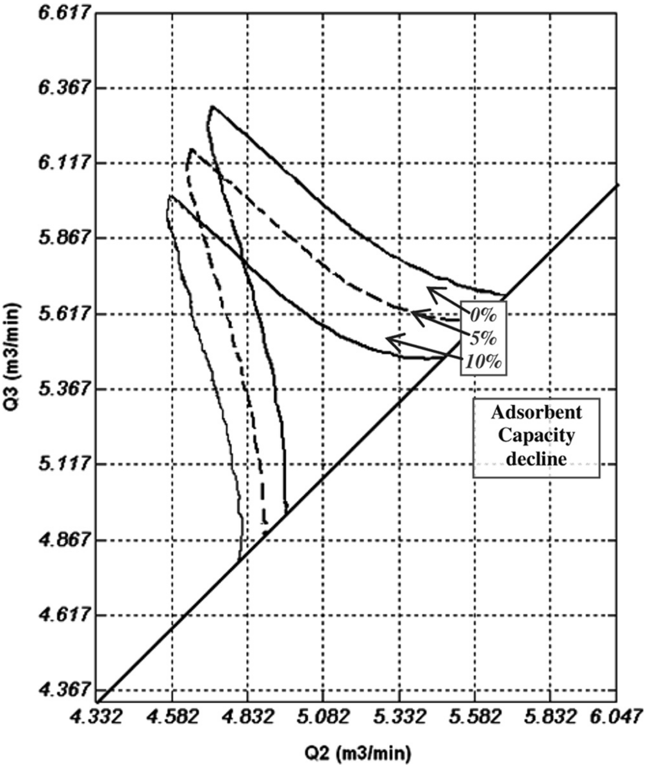

Figure 5. Adsorbent capacity decline influence on the separation region (purity over 99.50% of *p-xylene* in the extract and other C_8 isomers in the raffinate currents), where 0% represents the initial state adsorbent, 5% and 10% after 5% and 10% of adsorbent capacity decline respectively; all operating parameters kept constant as appointed in sub-section 2.4.1.

i, respectively, and $\overline{\langle x_{pi}\rangle}$ and $\overline{\langle C_p\rangle}$ obtained from:

$$Q_{Feed}C_i^F + Q_{De}C_i^D = \overline{\langle x_{pi}\rangle\langle C_p\rangle}(Q_{De} + Q_{Feed}), \text{ where } \sum_{i=1}^{NC}\overline{\langle x_{pi}\rangle} = 1.$$

$$\text{Giving}\begin{cases}\overline{\langle x_{pA}\rangle} = 0.105\\ \overline{\langle x_{pB}\rangle} = 0.222\\ \overline{\langle x_{pC}\rangle} = 0.058 \quad \text{and } \overline{\langle C_p\rangle} = 720.317\,\text{kg.m}^{-3}\\ \overline{\langle x_{pD}\rangle} = 0.063\\ \overline{\langle x_{pE}\rangle} = 0.552\end{cases}$$

leading to $\alpha = 1.8$. By optimization of the case study during 10 years (maximization of amount of p-xylene recovered in the extract with a purity value equal of higher than 99.5%), it was found that the value of α that better suits the switching time compensating measure is $\alpha = 3.2$.

Considering this α-value, it was possible to achieve at the end of the 10th year 1.4462 Mton (over a 10 years period) of p-xylene production (less 2.30% than with the fresh adsorbent unit) with *p-xylene* purity of 99.5% and recovery of 92.3% (Fig. 6).

One can observe in Fig. 6 that the effect noted in Fig. 4 was almost "corrected" by implementation of this compensating measure.

Variable Section Length Compensation

Using the operating conditions found for the Varicol mode of operation given in an earlier sub-section, now affected by 1% per year adsorbent capacity decline rate, it was implemented an optimization procedure to find the best column re-configuration during a period of 10 years. The optimization considers the maximization of p-xylene recovery in the extract above 99.5% purity rate by changing the column configuration in the last 5 years, *i.e.*, in the first 5 years the unit runs with the [5.6 7.4 6 5], the initial optimum, in the last 5 years with a different configuration (the variable section length countermeasure). With this approach it was possible to achieve at the end of the 10th year production of 1.3862 Mton of p-xylene (over a 10 years period) with an extended p-xylene purity of 99.5% and p-xylene recovery of 76.1%, the unit operates under [5.6 7.4 6 5] configuration in the first 5 years and [7.6 4.6 4.7 7.1] configuration in the 5 remaining ones (see Fig. 7). The obtained p-xylene productivity is lower for 8.80% than the one obtained with fresh adsorbent see (section on operating conditions found for the Varicol mode of operation) and higher for 1.70% in comparison with the Varicol unit running without any compensating measure.

As can be observed in Fig. 7, the columns in sections 2 and 3 moved to the regeneration ones (1 and 4), this evidence is easily stated with a better look on Fig. 4 (one should remind that the classic profiles are similar to the Varicol ones). With adsorbent capacity decline, the importance of the length of section 2 and 3 decreases and some plateaus are already seen (for instance, all species in section 3), showing that there is already some unused "column space."

Variable Section Length Compensation with Switching Time Compensation

Let us now implement the switching time compensating measure on the Varicol modus operandi (constant section lengths [5.6 7.4 6 5] during first

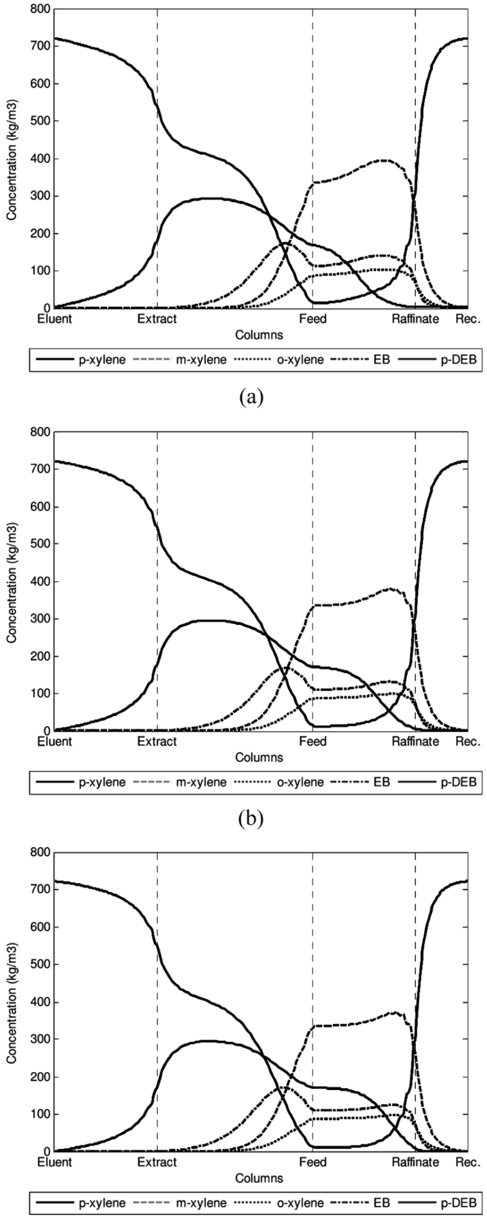

(a)

(b)

(c)

Figure 6. Concentration profiles evolution over a 10 years period without with the switching time compensating measure, (a) after 10 days, (b) after 5 years and (c) after 10 years.

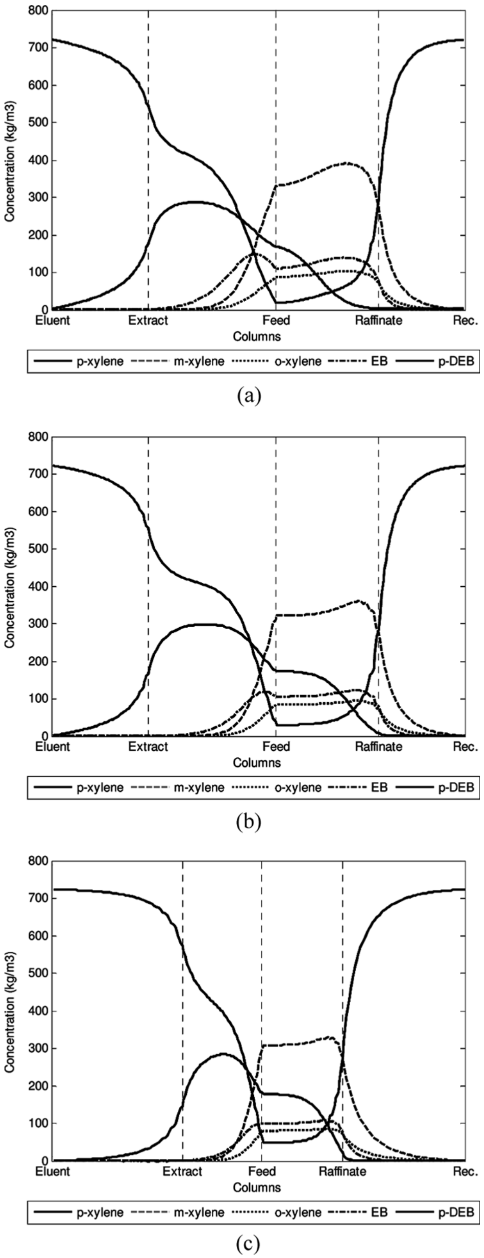

(a)

(b)

(c)

Figure 7. Concentration profiles evolution over a 10 years period with the switching time compensating measure, (a) after 10 days, (b) after 2.5 years and (c) after 7.5 years.

5 years and [7.6 4.6 4.7 7.1] in the 5 remaining ones) and the adsorbent capacity decline rate of 1% per year (for the sake of simplicity the α value was kept at 3.2, as for the classic operation, the sub-section is just a simple extension). With this unit it is possible to achieve in the end of the 10th year production of 1.487 Mton of p-xylene (over a 10 years period) for 2.2% less than when fresh adsorbent is used, but operating at the end of the 10 years period, with a p-xylene purity value of 99.4% and a recovery of 92.7%.

CONCLUSION

The operation of an industrial scale SMB unit for p-xylene separation in the presence of adsorbent ageing was studied. The standard SMB and the Varicol mode of operation were simulated accounting for the adsorbent capacity decline using the TMB approach. In the case of the Varicol unit, the noninteger number of columns per section was used in the simulations. Taking into account that p-xylene and its isomers are present in the system in high concentration, the model considered variable fluid velocity due to the adsorption/desorption rate. The effect of 1% per year on the adsorbent capacity decline was simulated over a 10 years period in a classic as well as in the Varicol unit. It was found that by the implementation of short cut countermeasures (switching time compensation and section length variation) it is possible to extended the adsorbent life under the minimum purity requirements. Nevertheless, the switching time measure leads to better productivity results than the variable section length, either when applied to the classic or to the Varicol modus operandi.

ACKNOWLEDGEMENTS

Pedro Sá Gomes acknowledges the financial support from FCT "Fundação para a Ciência e a Tecnologia" (Ph.D. grant SFRH/BD/22103/2005), Ministry of Science and Technology of Portugal and cooperation of Dr. Ping Li (ECUST, China) regarding Chinese literature references. Financial support through the project POCI/EQU/59296/2004 is gratefully acknowledged.

NOMENCLATURE

C_b	bulk fluid phase concentration $\mathrm{mol \cdot m^{-3}}$
C^F	feed concentration $\mathrm{mol \cdot m^{-3}}$

$\langle C_{pij} \rangle$	average pores particle adsorbent fluid phase concentration $\mathrm{mol} \cdot \mathrm{m}^{-3}{}_{\mathrm{solid}}$
D_{ax}	axial dispersion coefficient $\mathrm{m}^2 \cdot \mathrm{s}^{-1}$
D_c	column diameter m
k	particle mass transfer resistance coefficient s^{-1}
K	Langmuir adsorption constant $\mathrm{m}^3 \cdot \mathrm{kg}^{-1}{}_{\mathrm{solid}}$
L_c	column axial length m
n_j	number of columns per section
PU	purity %
PR	unit productivity $\mathrm{g} \cdot (\mathrm{s} \cdot \mathrm{m}^3{}_{\mathrm{realsolid}})^{-1}$
Q	fluid/solid flowrate $\mathrm{m}^3 \cdot \mathrm{s}^{-1}$
q^*	solid retained concentration $\mathrm{kg} \cdot \mathrm{kg}^{-1}{}_{\mathrm{solid}}$
$q_m{}^0$	initial solid retained concentration $\mathrm{kg} \cdot \mathrm{kg}^{-1}{}_{\mathrm{solid}}$
RE	recovery %
R_p	particle radius m
t	time variable s
t_s	solid space time (switching time) s
u_j	interstitial fluid velocity in a TMBR section $\mathrm{m} \cdot \mathrm{s}^{-1}$
u_s	solid interstitial counter-current velocity $\mathrm{m} \cdot \mathrm{s}^{-1}$
V_c	column volume m^3
z	axial column coordinate m

Greek Letters

α	porosity weight factor in the switching time compensating measure
ε_b	bed porosity
ε_p	particle porosity
ρ_p	solid density $\mathrm{kg} \cdot \mathrm{m}^{-3}$
ρ_f	fluid (liquid) density $\mathrm{kg} \cdot \mathrm{m}^{-3}$
ξ	adsorbent capacity decline rate $\% \cdot \mathrm{year}^{-1}$

Indexes

$*$	in the SMB unit (SMB model)
A	p-xylene
B	m-xylene
C	o-xylene
D	ethylbenzene
E	diethylbenzene
b	bulk
p	particle
s	solid
c	column
i	chemical species

j	TMB/SMB section
De	desorbent stream
F	feed stream
R	raffinate stream
X	extract stream

Abbreviations

AE	*Algebraic equations*
OCFEM	*Orthogonal Collocation in Finite Elements Method*
ODE	*Ordinary Differential Equations*
PDE	*Partial Differential Equations*
SMB	*Simulated Moving Bed*
TMB	*True Moving Bed*

REFERENCES

1. Broughton, D.B., Gerhold, C.G. (1961) Continuous Sorption Process Employing Fixed Bed of Sorbent and Moving Inlets and Outlets. US Patent no 2 985 589.
2. Ludemann-Hombourger, O., Nicoud, R.M., Bailly, M. (2000) 'VARICOL' process: A new multicolumn continuous chromatographic process. *Separation Science and Technology*, *35*: 1829–1862.
3. Jin, W., Wankat. P.C. (2005) Parallel two-zone and four-zone hybrid SMB system for the separation of P-xylene, in *AIChE Annual Meeting Conference Proceedings*.
4. Jin, W., Wankat, P.C. (2007) Hybrid simulated moving bed processes for the purification of p-xylene. *Separation Science and Technology*, *42*: 669–700.
5. Kurup, A.S., Hidajat, K., Ray, A.K. (2006) Comparative study of modified simulated moving bed systems at optimal conditions for the separation of ternary mixtures under nonideal conditions. *Industrial & Engineering Chemistry Research*, *45*: 3902–3915.
6. Kurup, A.S., Hidajat, K., Ray, A.K. (2006) Optimal operation of a Pseudo-SMB process for ternary separation under non-ideal conditions. *Separation and Purification Technology*, *51*: 387–403.
7. Minceva, M., Rodrigues, A.E. (2002) Modeling and simulation of a simulated moving bed for the separation of p-xylene. *Industrial and Engineering Chemistry Research*, *41*: 3454–3461.
8. Minceva, M., Rodrigues, A.E. (2003) Influence of the transfer line dead volume on the performance of an industrial scale simulated moving bed for p-xylene separation. *Separation Science and Technology*, *38*: 1463–1497.
9. Minceva, M., Rodrigues, A.E. (2004) Adsorption of xylenes on faujasite-type zeolite: Equilibrium and kinetics in batch adsorber. *Chemical Engineering Research and Design*, *82*: 667–681.

10. Minceva, M., Rodrigues, A.E. (2007) Understanding and revamping of industrial scale SMB units for p-xylene separation. *AIChE Journal*, *53*: 138–149.
11. Sá Gomes, P., Minceva, M., Rodrigues, A.E. (2007) Operation strategies for simulated moving bed in presence of adsorbent ageing. *Separation Science and Technology*, *42*: 1–37.
12. Pilliod, D.L., Randall, K.C., Harding, E.M. (2006) An Adsorption Process with on-line Adsorbent Removal. WO Patent no 118740 A1.
13. Pilliod, D.L., Randall, K.C., Harding, E.M. (2006) A Process for Hydrocarbon Conversion with on-line Solid Particulate Material Removal. WO Patent no 118739 A2.
14. Frey, S.J., Sechrist, P.A., Kauff, D.A. (2006) Fluid Distribution Apparatus. WO Patent no 055222 A1.
15. Natarajan, S., Lee, J.H. (2000) Repetitive model predictive control applied to a simulated moving bed chromatography system. *Computers and Chemical Engineering 7th International Symposium on Process Systems Engineering, Jul 16–Jul 21 2000*, *24*: 1127–1133.
16. Amanullah, M., Grossmann, C., Mazzotti, M., Morari, M., Morbidelli, M. (2007) Experimental implementation of automatic 'cycle to cycle' control of a chiral simulated moving bed separation. *Journal of Chromatography A*, *1165*: 100–108.
17. Toumi, A., Engell, S., Diehl, M., Bock, H.G., Schlöder, J. (2007) Efficient optimization of simulated moving bed processes. *Chemical Engineering and Processing: Process Intensification*, *46*: 1067–1084.
18. Santacesaria, E., Morbidelli, M., Danise, P., Mercenari, M., Carra, S. (1982) Separation of xylenes on Y zeolites. 1. Determination of the adsorption equilibrium parameters, selectivities, and mass transfer coefficients through finite bath experiments. *Industrial and Engineering Chemistry Process Design and Development*, *21*: 440–445.
19. Minceva, M. (2004) Separation/Isomerisation of Xylenes by Simulated Moving Bed Technology. *PhD Thesis, Porto Portugal.*
20. Neves, S.B. (1995) Modeling of Adsorption Fixed-bed in Liquid-solid Systems. M.Sc. Thesis Universidade Federal da Bahia, Brazil.
21. Minceva, M., Rodrigues, A.E. (2005) Two-level optimization of an existing SMB for p-xylene separation. *Computers and Chemical Engineering*, *29*: 2215–2228.
22. Kurup, A.S., Hidajat, K., Ray, A.K. (2005) Optimal operation of an industrial-scale parex process for the recovery of p-xylene from a mixture of C_8 aromatics. *Industrial and Engineering Chemistry Research*, *44*: 5703–5714.
23. Yu, F. (2004) Analysis of p-xylene adsorbent deactivation and the countermeasures. *Petroleum Refinery Engineering*, *34*: 46–48.
24. (2003) Successful regeneration of poisoned adsorbent for aromatics plant in Luoyang Petrochemical Company. *China Petroleum Processing and Petrochemical Technology*, Issue 1 *42*.
25. Methivier, A. (1998) Influence of oxygenated contaminants on the separation of C8 aromatics by adsorption on Faujasite zeolites. *Industrial and Engineering Chemistry Research*, *37*: 604–608.

APPENDIX

It was mentioned that a Varicol unit can be modelled by means of an equivalent TMB unit working with a non integer number of columns per section. In the limit, if one considers a Varicol unit with infinite number of columns and infinite number of sub-switching-intervals within the principal switching time interval, one should find the mentioned TMB unit (with noninteger number of columns per section, or different columns length).

To state this approach a Varicol unit was simulated by the real SMB approach (considering all Varicol discontinuities) and compared with an equivalent TMB with non integer number of columns. Thus, let us start to establish the real SMB model approach to the Varicol modus operandi. In this model various discontinuities are present, here classified in to categories:

1. With the principal switch, after each switching time all inlet/outlet ports suffer a synchronous shift for a “column length” in the fluid direction; and
2. With a sub-switch, within each principal switch period selected inlet/outlet ports (located between the variable length sections) suffer an asynchronous shift, either in the fluid or solid direction.

For the nodes equations for period 0 before the first sub-switch interval it becomes:

$$\textit{Desorbent node}\colon C_{bi(Nc,z=L_{Nc})} = \frac{u^*_{(1,z=0)}}{u^*_{(Nc,z=L_{Nc})}} C_{bi(1,x=0)} - \frac{u_{De}}{u^*_{(Nc,z=L_{Nc})}} C_i^{De} \tag{A1a}$$

$$\textit{Extract, Raffinate and columns nodes}\colon C_{bi(k-1,z=L_{k-1})} = C_{bi(k,z=0)} \tag{A1b}$$

$$\begin{aligned}\textit{Feed node}\colon C_{bi(n_1+n_2,z=L_{n_1+n_2})} = {} & \frac{u^*_{(n_1+n_2+1,z=0)}}{u^*_{(n_1+n_2,z=L_{n_1+n_2})}} C_{bi(n_1+n_2+1,z=0)} \\ & - \frac{u_F}{u^*_{(n_1+n_2,z=L_{n_1+n_2})}} C_i^F\end{aligned} \tag{A1c}$$

and,

$$u^*_{(1,z=0)} = u^*_{(Nc,z=L_{Nc})} + u_{De} \qquad \textit{Desorbent}(De)\ \textit{node}; \tag{A2a}$$

$$u^*_{(n_1+1,z=0)} = u^*_{(n_1,z=L_{n_1})} - u_X \qquad \textit{Extract}(X)\ \textit{node}; \tag{A2b}$$

$$u^*_{(n_1+n_2+1,z=0)} = u^*_{(n_2+n_1,z=L_{n_2+n_1})} + u_F \qquad \textit{Feed}(F)\ \textit{node}; \tag{A2c}$$

$$u^*_{(n_1+n_2+n_3+1,z=0)} = u^*_{(n_1+n_2+n_3,z=Ln_1+n_2+n_3)} - u_R \qquad \textit{Raffinate}(R)\ \textit{node}. \tag{A2d}$$

$$u^*_{(k,z=0)} = u^*_{(k-1,z=L_{k-1})} \qquad \textit{The remaining columns}. \tag{A2e}$$

In our case, a Varicol unit working with $n_j = [5\ 7\ 7\ 5]$ from 0 to $0.4t_s$ and $n_j = [6\ 6\ 7\ 5]$ from $0.4t_s$, there is only 1 sub-switch occurring $0.4t_s$ after the principal switch, shifting the extract port in fluid direction. In period 0 after this first sub-switch just Eq. (A2b) is actualized all the rest remains the ones above.

After the first principal switch Eqs. (A1) and (A2) become:

$$\textit{Desorbent node}\colon C_{bi(1,z=L_1)} = \frac{u^*_{(2,z=0)}}{u^*_{(1,z=L_1)}} C_{bi(2,x=0)} - \frac{u_{De}}{u^*_{(1,z=L_1)}} C_i^{De} \tag{A1a*}$$

$$\textit{Extract, Raffinate and columns nodes}\colon C_{bi(k-1,z=L_{k-1})} = C_{bi(k,z=0)} \tag{A1b*}$$

$$\begin{aligned}\textit{Feed node}\colon & C_{bi(n_1+n_2+1,z=L_{n_1+n_2+1})} \\ & = \frac{u^*_{(n_1+n_2+2,z=0)}}{u^*_{(n_1+n_2+1,z=L_{n_1+n_{2+1}})}} C_{bi(n_1+n_2+2,z=0)} \\ & - \frac{u_F}{u^*_{(n_1+n_2+1,z=L_{n_1+n_{2+1}})}} C_i^F\end{aligned} \tag{A1c*}$$

and,

$$u^*_{(2,z=0)} = u^*_{(1,z=L_1)} + u_{De} \qquad \textit{Desorbent}(De)\ \textit{node}; \tag{A2a*}$$

$$u^*_{(n_1+2,z=0)} = u^*_{(n_1+1,z=L_{n_1+1})} - u_X \qquad \textit{Extract}(X)\ \textit{node}; \tag{A2b*}$$

$$u^*_{(n_1+n_2+2,z=0)} = u^*_{(n_2+n_1+1,z=L_{n_2+n_1+1})} + u_F \qquad \textit{Feed}(F)\ \textit{node}; \tag{A2c*}$$

$$\begin{aligned} u^*_{(n_1+n_2+n_3+2,z=0)} &= u^*_{(n_1+n_2+n_3+1,z=Ln_1+n_2+n_3+1)} - u_R \\ & \qquad \textit{Raffinate}\ (R)\ \textit{node}.\end{aligned} \tag{A2d*}$$

$$u^*_{(k,z=0)} = u^*_{(k-1,z=L_{k-1})} \qquad \textit{The remaining columns.} \qquad (\text{A2e}^*\text{a})$$

$$u^*_{(1,z=0)} = u^*_{(Nc,z=L_{Nc})} \qquad \textit{The recycle connection.} \qquad (\text{A2e}^*\text{b})$$

this periodical procedure continues similarly until the complete cycle and then restarts again.

Then performing the species mass balances, considering a convective axial dispersed liquid flux with variable velocity flowing, homogeneous particles with constant radius R_P, constant axial dispersion, and intraparticle mass transfer resistances. Negligible pressure drops as negligible thermal effects. It becomes:

for the bulk fluid, in column k:

$$\frac{\partial C_{bik}}{\partial t} = D_{ax}\frac{\partial^2 C_{bik}}{\partial z^2} - \frac{\partial(C_{bik}u^*_k)}{\partial z} - \frac{(1-\varepsilon_b)}{\varepsilon_b}k_{ik}(C_{bik} - \langle C_{pik}\rangle) \qquad (\text{A3})$$

and for "solid phase":

$$\rho_p\frac{\partial q_{ik}}{\partial t} + \varepsilon_p\frac{\partial\langle C_{pik}\rangle}{\partial t} = k_{ik}(C_{bik} - \langle C_{pik}\rangle) \qquad (\text{A4})$$

with the initial and boundary conditions:

$$\begin{cases} C_{bik}(z,0) = 0; \\ \langle C_{pik}(z,0)\rangle = 0; \quad i = (A,B,C,D) \text{ and} \\ \langle q_{ik}(z,0)\rangle = 0; \end{cases} \begin{cases} C_{bEk}(z,0) = \rho_E; \\ \langle C_{pEk}(z,0)\rangle = \rho_E; \\ \langle q_{Ek}(z,0)\rangle \cong q_{m_E}; \end{cases} \qquad (\text{A5})$$

$$z = 0 : C_{bi(k,z=0)} = C_{bik}(0,t) - \frac{D_{ax}}{u^*_k}\frac{\partial C_{bik}}{\partial z}\bigg|_{z=0} \qquad (\text{A6})$$

$$z = L_k : \frac{\partial C_{bik}}{\partial z}\bigg|_{z=L_k} = 0 \qquad (\text{A7})$$

The adsorption equilibrium isotherm defined as:

$$q^*_{ik} = f_i(C_{pik}, C_{plk}) \text{ with } l \neq i \text{ and for all species } i \text{ and in column } k \qquad (\text{A8})$$

And considering that:

$$\sum_{i=1}^{NC}\frac{C_{bik}}{\rho_i} = 1$$

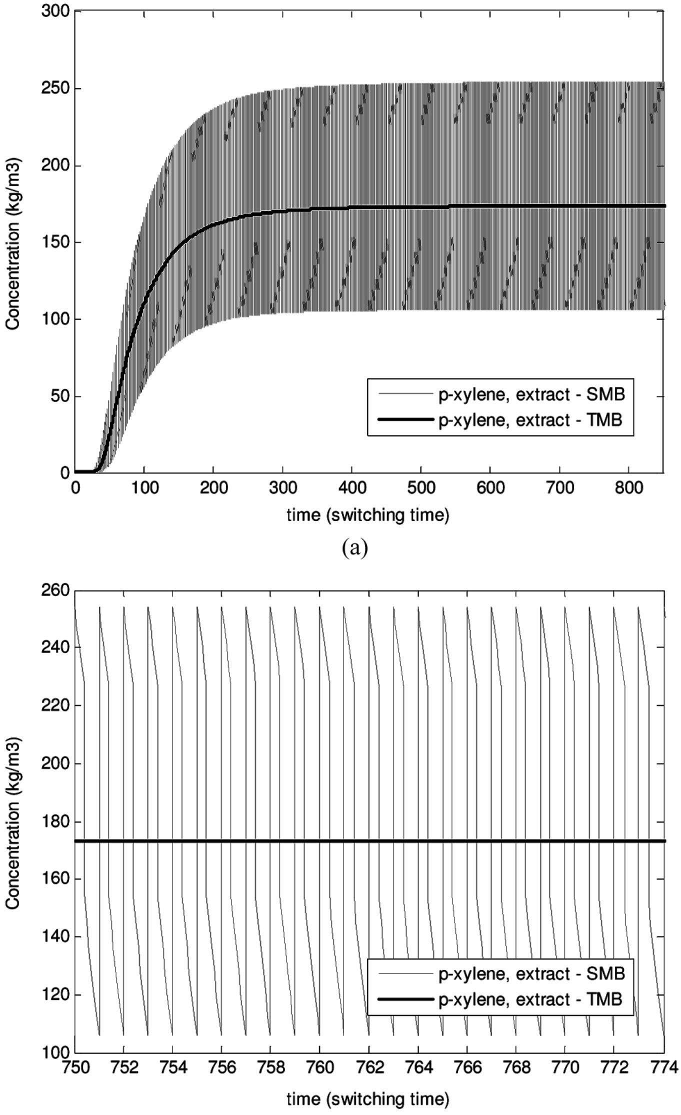

(a)

(b)

Figure A1. *p-xylene* concentration profiles in the extract current for Varicol modus operandi, modelled by SMB and the equivalent TMB, (a) until cyclic steady state, and (b) the detail over a cycle in the cyclic steady state.

Table A1. Extract concentrations for the SMB and TMB model approaches to the Varicol

	Concentration (kg.m^{-3})			
	p-xylene	o-xylene	m-xylene	EB
Varicol-SMB	173.56	0.30	0.08	0.54
Varicol-TMB	173.75	0.27	0.07	0.50
$\frac{Cb_i^{SMB}-Cb_i^{TMB}}{Cb_I^{SMB}}$ (%)	0.11	10.00	12.50	7.41
$\frac{Cb_i^{SMB}-Cb_i^{TMB}}{Cb_{p-xylene}^{SMB}}$ (%)	0.11	0.02	0.01	0.02
$PUX^A{}_{TMB}$ (%)	99.51	$PUX^A{}_{SMB}$ (%)	99.47	

Table A2. Raffinate concentrations for the SMB and TMB model approaches to the Varicol

	Concentration (kg.m^{-3})			
	p-xylene	o-xylene	m-xylene	EB
Varicol-SMB	3.17	278.11	73.01	78.25
Varicol-TMB	3.02	278.16	73.02	78.28
$\frac{Cb_i^{SMB}-Cb_i^{TMB}}{Cb_i^{SMB}}$ (%)	4.43	−0.02	−0.01	−0.04
$\frac{Cb_i^{SMB}-Cb_i^{TMB}}{Cb_{o-xylene}^{SMB}+Cb_{m-xylene}^{SMB}+Cb_{EB}^{SMB}}$ (%)	0.03	−0.01	<0.01	−0.01

It is possible to calculate the interstitial fluid velocity by means of the total mass balance, becoming:

$$\frac{du_k^*}{dz} = -\frac{(1-\varepsilon_b)}{\varepsilon_b}\sum_{i=1}^{NC}\frac{k_{ik}}{\rho_i}\left(C_{bik} - \langle C_{pik}\rangle\right) \tag{A9}$$

with exception to the columns distribution: $n_j = [5\ 7\ 7\ 5]$ from 0 to $0.4t_s$ and $n_j = [6\ 6\ 7\ 5]$ from $0.4t_s$ to t_s, and recycle flowrate ($Q_{Rec}{}^* = 619.93\,\mathrm{m}^3 \cdot \mathrm{h}^{-1}$), the same operating conditions set on the section on the optimization of varicol SMB unit were used. The p-xylene concentration profile in the extract current are presented in Fig. A1, for outlet concentration in Tables A1 and A2, by SMB and the equivalent TMB, (a) until cyclic steady state, and (b) the detail over a cycle in the cyclic steady state.

One should take into account that the observed impurities differences (o-xylene, m-xylene, and EB in the extract current or p-xylene in the raffinate one), are not significant, they appear as residuals, as a result it is present a corrected deviation: $Cb_i^{SMB} - Cb_i^{TMB} / Cb_{p-xylene}^{SMB}$ in the extract and $Cb_i^{SMB} - Cb_i^{TMB} / Cb_{o-xylene}^{SMB} + Cb_{m-xylene}^{SMB} + Cb_{EB}^{SMB}$ in the raffinate current, to better compare both approaches.

As can be noted the results are quite similar, and the relative deviations near to the ones obtained with classical modes of operation modelled by SMB or equivalent TMB.